

Fourier Transform with
Rotations on Circles
and Ellipses
in Signal and Image Processing

Artyom M. Grigoryan
Department of Electrical and Computer Engineering
University of Texas at San Antonio One UTSA Circle,
San Antonio, USA TX 78249
e-mail: amgrigoryan@utsa.edu

Introduction

We analyze the general concept of rotation and processing of data around not only circles but ellipses, in general. The general concept of the elliptic Fourier transform which was developed by [Grigoryan, 2009]. The block-wise representation of the discrete Fourier transform (DFT) is considered in the real space, which is effective and that can be generalized to obtain new methods in spectral analysis. The N -point Elliptic DFT (EDFT) uses as a basic 2×2 transformation the rotations around ellipses.

The EDFT distinguishes well from the carrying frequencies of the signal in both real and imaginary parts. It also has a simple inverse matrix. It is parameterized and includes also the DFT. Our preliminary results show that by using different parameters, the EDFT can be used effectively for solving many problems in signal and image processing field, in which includes problems such as image enhancement, filtration, encryption and many others.

DFT in the real space

The DFT of the signal $\mathbf{f} = (f_0, f_1, f_2, \dots, f_{N-1})'$

$$F_p = R_p + iI_p = \sum_{n=0}^{N-1} W^{np} f_n, \quad p = 0 : (N-1).$$

The matrix in the complex space C^N is

$$[\mathcal{F}_N] = \begin{bmatrix} 1 & 1 & 1 & 1 & 1 & 1 \\ 1 & W^1 & W^2 & W^3 & \dots & W^{N-1} \\ 1 & W^2 & W^4 & W^6 & \dots & W^{N-2} \\ 1 & \dots & \dots & \dots & \dots & \dots \\ 1 & \dots & \dots & \dots & \dots & \dots \\ 1 & W^{N-1} & W^{N-2} & W^{N-3} & \dots & W^1 \end{bmatrix}$$

Here, by N roots $W^k = W_N^k$ of the unit are

$$W^k = e^{-i\frac{2\pi}{N}k} = c_k - is_k = \cos\left(\frac{2\pi}{N}k\right) - i \sin\left(\frac{2\pi}{N}k\right)$$

$k = 0 : (N-1)$. Thus, the N -point discrete Fourier transform of the signal is defined as a decomposition of the signal by N roots located on the unit circle, $(W^k)^N = 1$.

We describe the multiplication of the complex number in matrix form. The input signal, or vector $\mathbf{x} = x_1 + ix_2$ which is $(x_1, x_2)'$ is multiplied by the coefficients W^k ,

$$\mathbf{x} = \begin{pmatrix} x_1 \\ x_2 \end{pmatrix} \rightarrow W^k \mathbf{x} = \begin{pmatrix} c_k x_1 + s_k x_2 \\ c_k x_2 - s_k x_1 \end{pmatrix},$$

where $W^k = (c_k, -s_k) = \cos \varphi_k - i \sin \varphi_k$, and $\varphi_k = 2\pi k/N$.

In matrix form, this multiplication is

$$T^k \mathbf{x} = \begin{pmatrix} \cos \varphi_k & \sin \varphi_k \\ -\sin \varphi_k & \cos \varphi_k \end{pmatrix} \begin{pmatrix} x_1 \\ x_2 \end{pmatrix}.$$

The matrix of rotation by the angle $\varphi_k = k\varphi_1$ is denoted by T^k . ($k = 0 \rightarrow \varphi_0 = 0, T = I$)

Thus we transfer the complex plane into the 2-D real space, $C \rightarrow R^2$, and consider each operation of multiplication by the twiddle coefficient as the elementary rotation, or the Givens transformation, $W^k \rightarrow T^k, k = 0 : (N - 1)$.

The inclusion of the complex space $C^N \rightarrow R^{2N}$:

$$\mathbf{f} = (f_0, \dots, f_{N-1})' \rightarrow \bar{\mathbf{f}} = (r_0, i_0, \dots, r_{N-1}, i_{N-1})'$$

where we denote $r_k = \text{Re}f_k$ and $i_k = \text{Im}f_k$ for $k = 0 : (N - 1)$. The vector $\bar{\mathbf{f}}$ is composed from the original vector, or signal \mathbf{f} , and its vector-component is denoted by $\bar{\mathbf{f}}_k = (\bar{f}_{2k}, \bar{f}_{2k+1})' = (r_k, i_k)'$.

The N -point DFT of \mathbf{f} is represented in R^{2N} as the $2N$ -point transform

$$\bar{\mathbf{F}}_p = \begin{bmatrix} R_p \\ I_p \end{bmatrix} = \sum_{k=0}^{N-1} T^{kp} \bar{\mathbf{f}}_k = \sum_{k=0}^{N-1} T^{kp} \begin{bmatrix} r_k \\ i_k \end{bmatrix}$$

where $p = 0 : (N - 1)$.

The matrix of the DFT in the space R^{2N}

$$X = \begin{bmatrix} I & I & I & I & I & I \\ I & T^1 & T^2 & T^3 & \dots & T^{N-1} \\ I & T^2 & T^4 & T^6 & \dots & T^{N-2} \\ I & \dots & \dots & \dots & \dots & \dots \\ I & T^{N-1} & T^{N-2} & T^{N-3} & \dots & T^1 \end{bmatrix}.$$

The (n, p) -th blocks 2×2 of this matrix is T^{np} , where $n, p = 0 : (N - 1)$. The matrix $I = I_2$ is the identity matrix 2×2 .

When calculating the component of the DFT at the frequency-point p , the vector-components (r_k, i_k) as points are rotated by the corresponding angles $k\varphi_p$.

Thus the first point (r_0, i_0) stays on its place, the second point (r_1, i_1) is rotated around the circle of radius $\sqrt{r_1^2 + i_1^2}$ by angle φ_p . The next point (r_2, i_2) is rotated around the circle of radius $\sqrt{r_2^2 + i_2^2}$ by twice larger angle $2\varphi_p$, or twice faster, than the point (r_1, i_1) , and so on. Then the coordinates of all rotated points are added and one point is defined, which represents the DFT at frequency-point p .

For frequency-point $p = 0$, or F_0 , there is no rotation; the sums of coordinates of the original points define the component F_0 .

Example 1: Consider the vector-signal of length 10 with the following real and imaginary parts:

$$\{r_k; k = 0 : 9\} = \{5, -3, 2, -5, -1, 3, -4, -2, 7, -6\}$$

$$\{i_k; k = 0 : 9\} = \{-2, 1, 4, -3, 7, 2, -5, 5, -1, 3\}.$$

This signal is plotted in form of ten points on the plane in the figure. The points are numbered and ten circles on which they lie are shown.

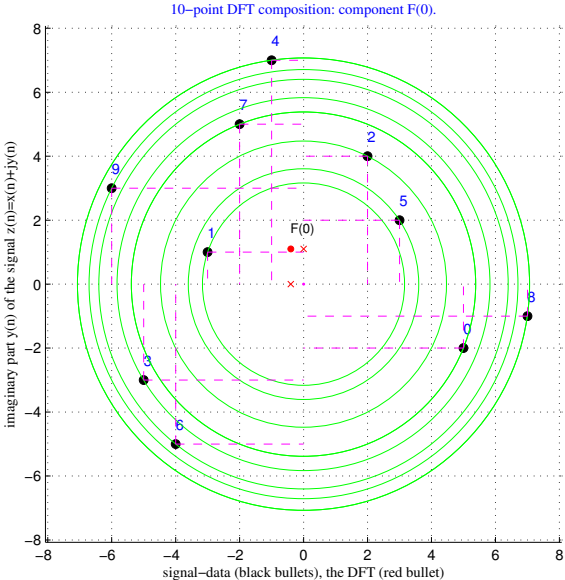


Figure shows projections of all points of the signal on the X-axis and Y-axis (shown by dash lines) and their sums (by x), and the point $F_0 = (-0.4, 1.1)$ (by the red bullet). On the next stage of the DFT calculation, points of the signals are rotated as shown in the right, and the sums of projections of the rotated points on the X-axis and Y-axis define the point $F_1 = (0.0684, -0.6155)$.

Similarly, these ten points are rotated eight more times, and during these rotations the sums of coordinates of ten points lie down on a new set of ten points with the following coordinates:

$$\{R_p\} = \{-0.4, 0.0684, 0.7729, \dots, -0.3618, 0.6733\}$$

$$\{I_p\} = \{1.1, -0.6155, -0.3367, \dots, -0.1015, 0.2009\}$$

These ten points $F_p = (R_p, I_p)$ are show in Figure 2.

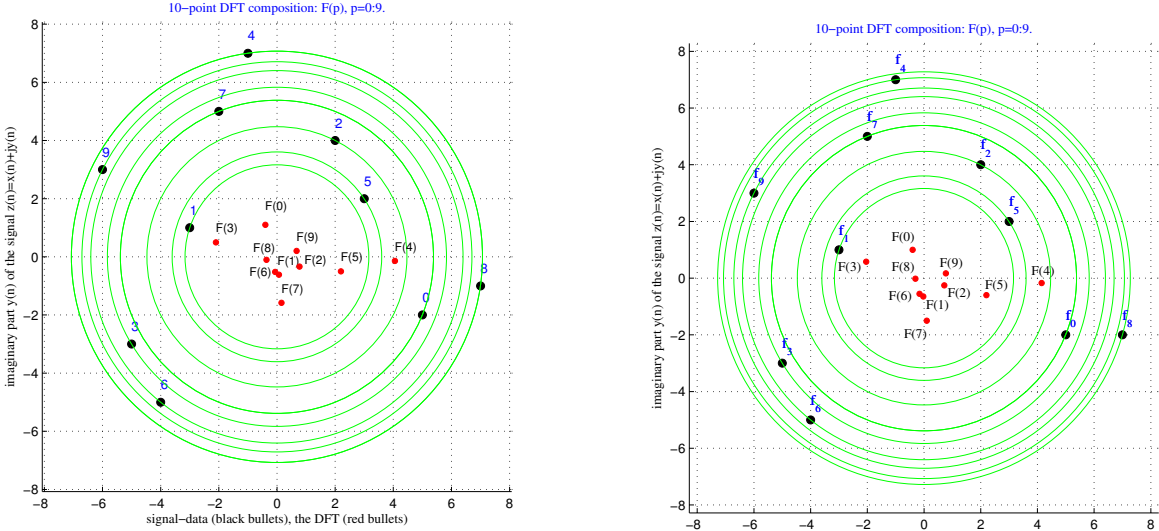


Figure 2. Result of ten rotations.

The system of rotation in the Inverse DFT is similar to the DFT, with the following difference. The IDFT is defined by rotation in the direction opposite to the rotation in the DFT. After rotating of the points, the sums of the coordinates of rotated points are normalized by the factor of N .

DFT and Horoscope

Consider the following symmetric complex signal f_n :

$$f_n = r_n + ji_n = n + j(n/5), \quad f_{-n} = f_n, \quad n = 0 : 200.$$

Next figures illustrate the geometry of a few components F_p of the 201-point DFT.

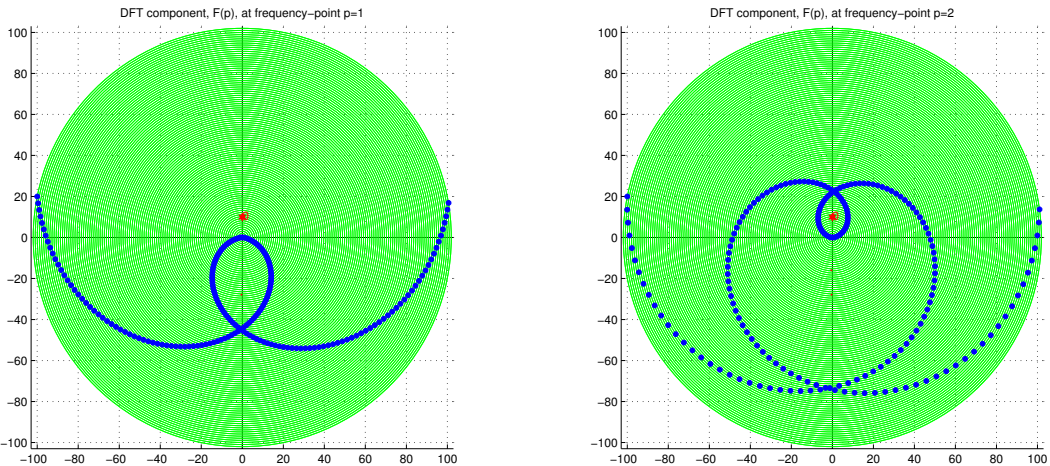


Figure 3. DFT components F_1 and F_2 .

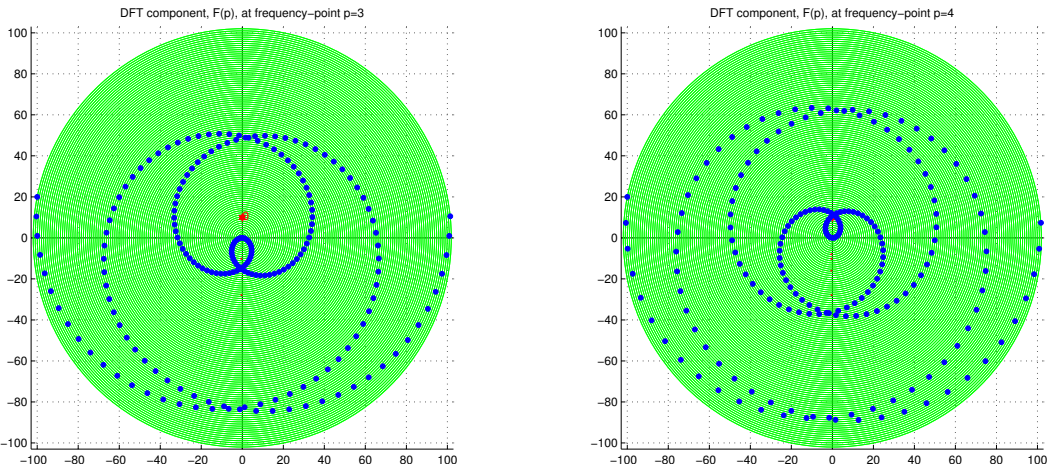


Figure 4. DFT components F_3 and F_4 .

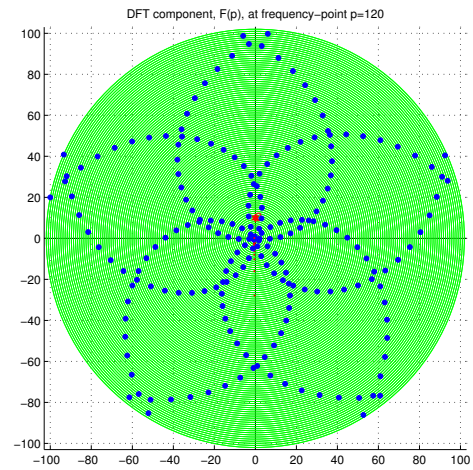
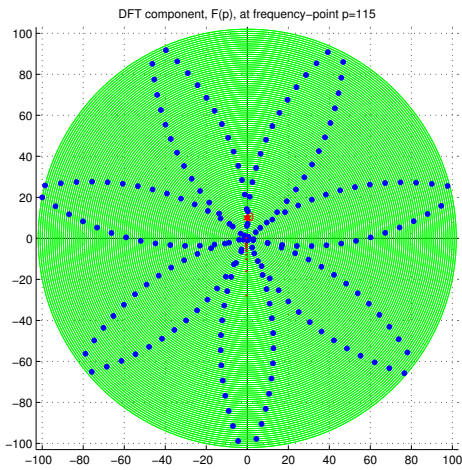


Figure 5. DFT components F_{115} and F_{120} .

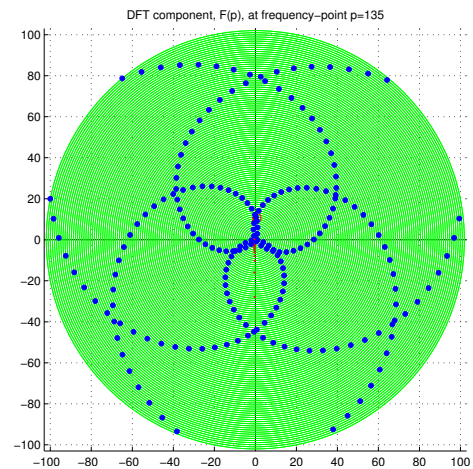
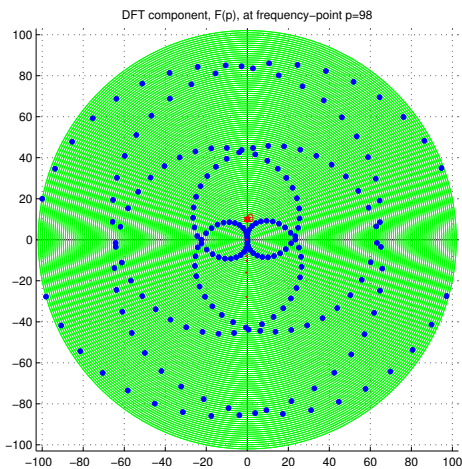


Figure 7. DFT components F_{98} and F_{135} .

Elliptic DFT

We consider the concept of the N th roots of the identity matrix 2×2 [Grigoryan 2006]. These basic transformations are defined by transformations different from the Givens rotations.

A new class of parameterized transformations which are called *elliptic-type I discrete Fourier transformations* are defined in the following way.

Given an integer $N > 1$ and angle $\varphi = \varphi_N = 2\pi/N$, the following matrix is considered:

$$C = C(\varphi) = \begin{bmatrix} \cos \varphi & \cos \varphi - 1 \\ \cos \varphi + 1 & \cos \varphi \end{bmatrix}.$$

This matrix can be written as

$$C = C(\varphi) = \cos \varphi \cdot U + V = \cos \varphi \begin{bmatrix} 1 & 1 \\ 1 & 1 \end{bmatrix} + \begin{bmatrix} 0 & -1 \\ 1 & 0 \end{bmatrix},$$

or $C = \cos \varphi \cdot I + \sin \varphi \cdot R$, where

$$R = R(\varphi) = \begin{bmatrix} 0 & -\tan(\varphi/2) \\ \cot(\varphi/2) & 0 \end{bmatrix}, \quad (\det R = 1).$$

This definition leads to the equality $C^N(\varphi) = I$ for any integer N , even or odd. The matrix R satisfies the condition $R^2(\varphi) = -I$.

For the $N = 5$ case, the matrix

$$C = C_{\frac{2\pi}{5}} = \begin{bmatrix} 0.3090 & -0.6910 \\ 1.3090 & 0.3090 \end{bmatrix}, \quad \det C = 1.$$

We consider the orbit of a point $\mathbf{x} = (1, 0)'$ with respect to the group of motion $\mathbf{C} = \{C^k; k = 0 : 4\}$, i.e., the movement of the point in the plane

$$\mathbf{x} \rightarrow C\mathbf{x} \rightarrow C^2\mathbf{x} \rightarrow C^3(\mathbf{x}) \rightarrow C^4(\mathbf{x}) \rightarrow C^5(\mathbf{x}) = \mathbf{x}.$$

These points $\mathbf{y}_k = C^k(\mathbf{x})$, $k = 0 : 4$, are on an ellipse.

If instead of C we consider the matrix of rotation W by the angle $\varphi = 2\pi/5$, then the point \mathbf{x} will move around a circle. The value of $\Delta(\varphi) = |b| - 1$ is be considered as a measure of difference of the elliptic and traditional discrete Fourier transformations.

For the considered above $N = 10$ case, Figure 8 shows the result of N rotations of these points when using the EDFT over the same signal.

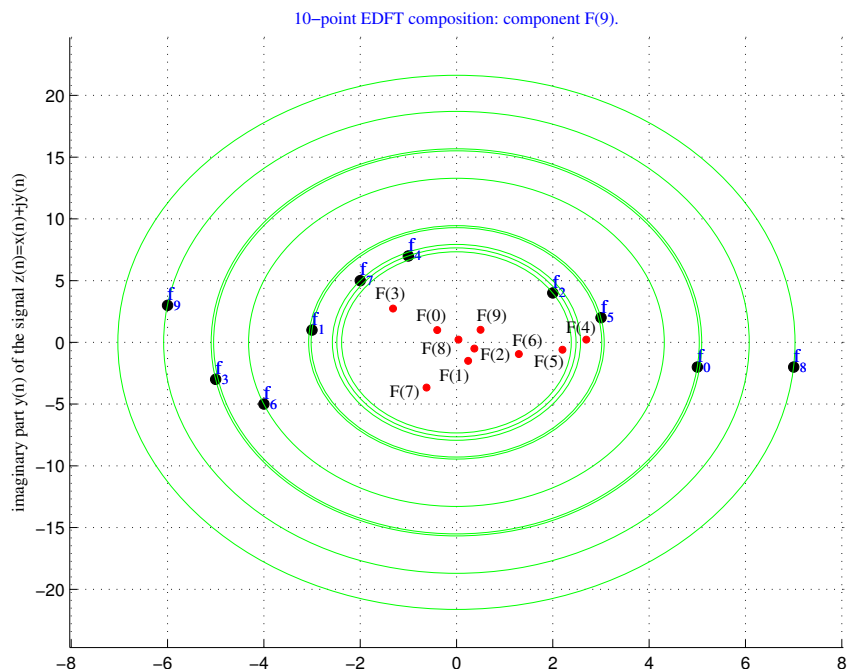


Figure 8. Signal rotation in the EDFT system.

To illustrate the difference between the EDFT and DFT, Figures 9-11 show geometry of a few components F_p calculated by the DFT and EDFT when the 128-point signal is the sampled sine wave

$$f(t) = 5 \sin(t), \quad t \in [-\pi, \pi].$$

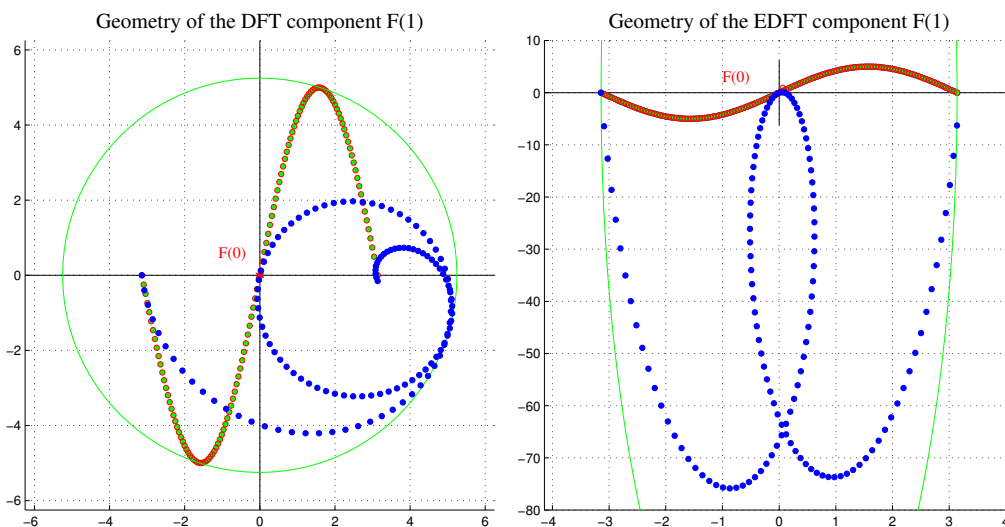


Figure 9. Geometry of the component F_1 in the DFT- and EDFT-systems of rotation.

The rotated values of the sine wave are shown together with the sine wave.

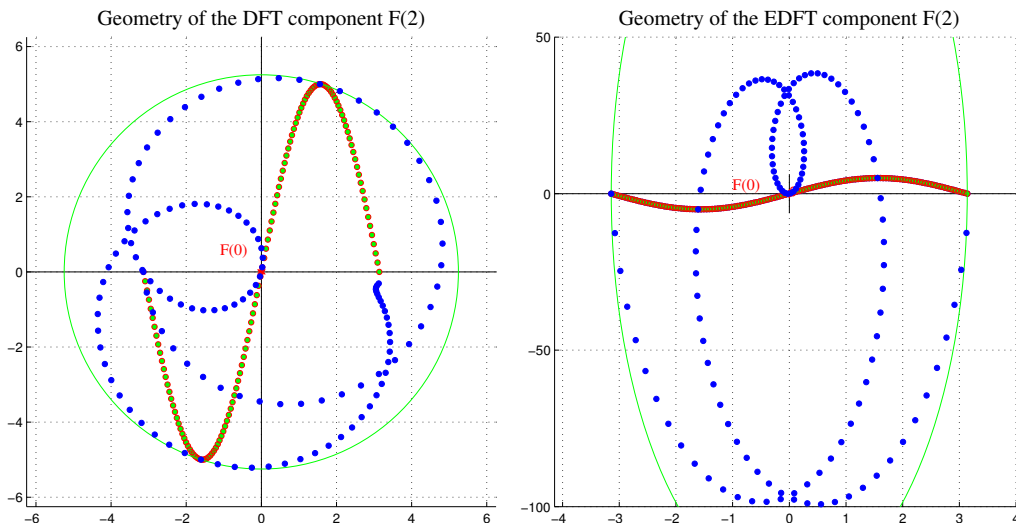


Figure 10. Geometry of the component F_2 in the DFT- and EDFT-systems of rotation.

The sine wave is rotated inside the circle of radius 5 when using the DFT. The EDFT rotate these data inside the ellipse.

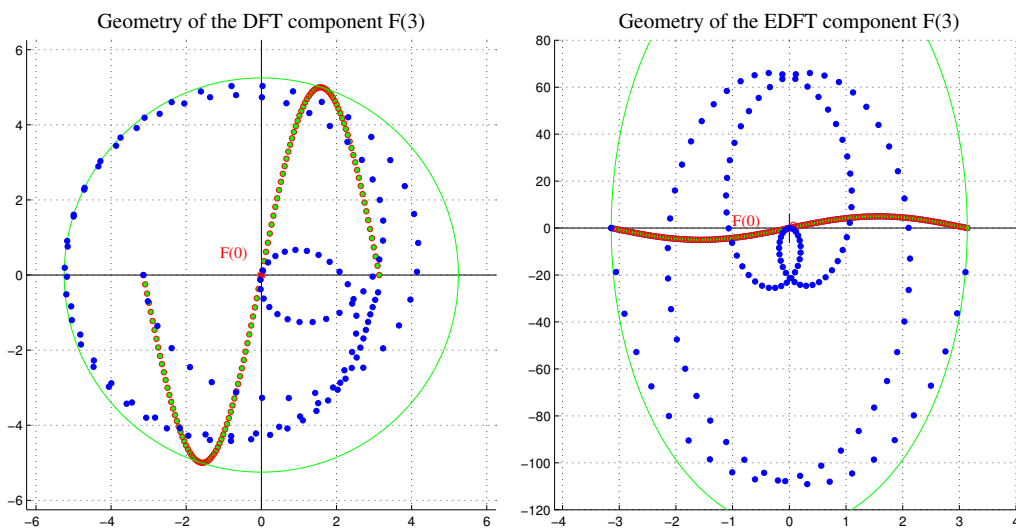


Figure 11. Geometry of the component F_3 in the DFT- and EDFT-systems of rotation.

EDFT in signal processing

One of the interesting properties of the elliptic Fourier transform is the fact that this transform can better distinguish the frequencies of the cosine or sine waves than the traditional transform.

Example 5:

Consider the $N = 120$ case. x_r is the following discrete-time cosine wave with low frequency $\omega_0 = 2\pi/N$ in the time interval $[0, 2\pi]$:

$$x_r(t) = 4 \cos(2\omega_0 t) + 0.2 \sin(6\omega_0 t) - 3 \cos(15\omega_0 t) - 0.05 \sin(9\omega_0 t).$$

The $2N$ -dimensional vector is composed as

$$\bar{x} = (x_r(0), 0, x_r(t_1), 0, x_r(t_2), 0, \dots, 0, x_r(t_{N-1}), 0)'$$

Figure 12 shows the discrete-time signal x_r in part a and the “real” part y_r of the 120-block EFT in b.

The basic transform equals

$$C = C(2\pi/128) = \begin{bmatrix} 0.9986 & -0.0014 \\ 1.9986 & 0.9986 \end{bmatrix}.$$

Figure 13 shows the discrete-time signal x in part a. The transforms DFT and EDFT of this signals are shown in parts b and c, respectively, in absolute mode.

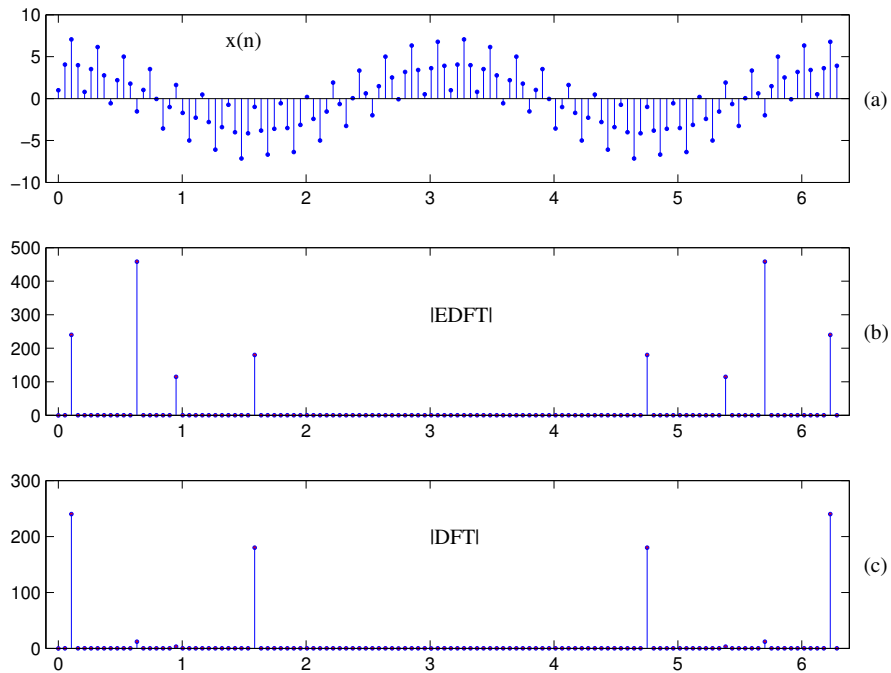


Figure 12. (a) The signal $f(t)$ with four carrier frequencies, and the magnitude of the (b) 120-block EDFT and (c) 120-block DFT of the signal.

In the frequency-points $p = 2$ and 15 , as well as in points $118 = 120 - 2$ and $105 = 120 - 15$, the traditional DFT recognizes well only two frequencies $2\omega_0$ and $15\omega_0$, because of high amplitudes of the carrier cosine waves $\cos(2\omega_0 t)$ and $\cos(15\omega_0 t)$ in $f(t)$. The amplitudes of other two sinusoidal waves $\sin(6\omega_0 t)$ and $\sin(9\omega_0 t)$ are small, and it is very difficult to notice these frequencies in the DFT. In contrary, the EDFT recognizes well all four frequencies $2\omega_0, 6\omega_0, 9\omega_0$, and $15\omega_0$, in the frequency-points $p = 2, 6, 9, 15$ and $118, 114, 111, 105$, respectively.

These frequencies have been enhanced in the “imaginary” part of the N -block EDFT of the signal. Figure 14 shows the “real” part of the N -block EDFT (or DFT) of the signal in part a, along with the “imaginary” part of the EDFT in b.

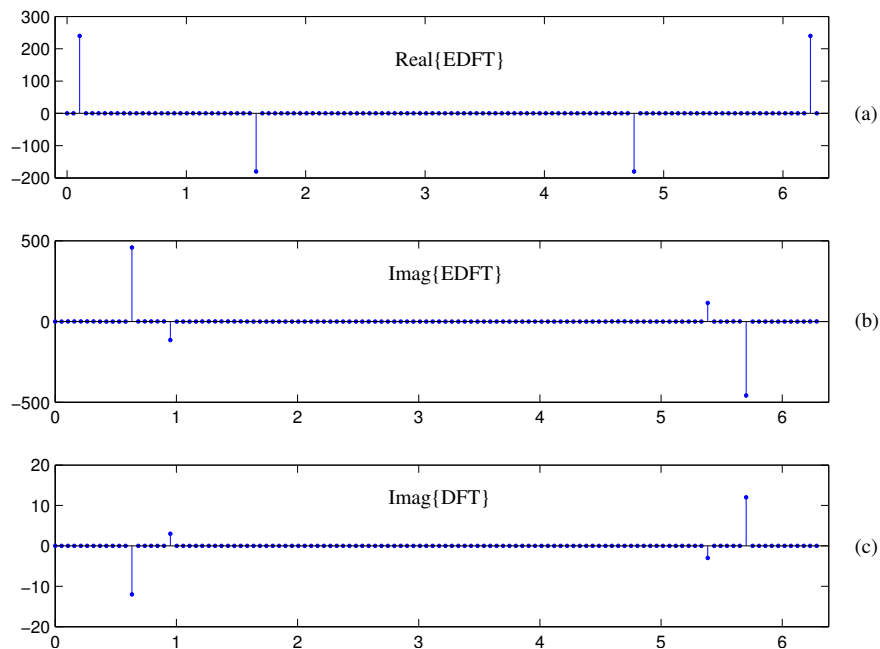


Figure 14. (a) The “real” part and (b) “imaginary” part of the 120-block EDFT of the signal, and (c) the imaginary part of the 120-block DFT of the signal.

For comparison, the imaginary part of the DFT is given in c. The imaginary part of the DFT by amplitude is smaller than the EDFT. The “imaginary” part of the EDFT enhances the magnitudes in these frequencies by factor of 31.8205 each.

EDFT in image processing

The EDFT has a unique and fast algorithm which can be applied for signals of any size. This transform can be used in image processing in filtering, enhancement, cryptography, and other applications in imaging. We consider the image enhancement by the EDFT with the following example.

Figure 15 shows the bridge image in part a. The image size is 256×256 , and we perform the 2-D separable EDFT by processing the rows and then columns by the 1-D 256-block EDFT with parameter $\varphi_1 = \pi/6 = 0.5236$. The inverse EDFT is calculated with values of φ which are different from φ_1 . First, we calculate the inverse 2-D separable EDFT by processing the columns and rows by the inverse 1-D 256-block EDFT with parameter $\varphi_2 = 0.6545$. The result of the inverse EDFT is an enhanced image which is shown in b. In part c, the enhanced image corresponds to the case when the inverse EDFT is calculated with parameter $\varphi_2 = 0.7330$.

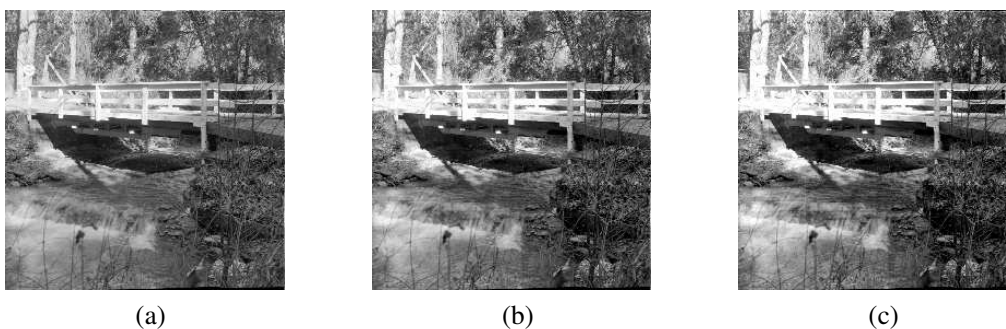


Figure 15. (a) The bridge image and the inverse φ_2 -defined 2-D EDFTs of the φ_1 -defined 2-D EDFT of the image when φ_2 is (b) 0.6545 and (c) 0.7330.

The elliptic DFT can also be used for enhancement of color images. As an example, we consider the Aivazovsky's image of the battle on the sea in Figure 16 in part a. The size of the image is 428×428 . The 2-D separable EDFT by processing the rows and then columns was calculated by the 1-D 428-block EDFT with parameter $\varphi_1 = \pi/6 = 0.5236$ over each color channel. The image is in the RGB color space. The inverse EDFT was calculated with values of $\varphi = \varphi_2 = 0.6545 \neq \varphi_1$. The result of this inverse EDFT is an enhanced image shown in b.



Figure 16. (a) The color image and the inverse φ_2 -defined 2-D EDFTs of the φ_1 -defined 2-D EDFT of the image when φ_2 is (b) 0.6545

In both given cases, the enhancement of the images have been performed by two different EDFTs, namely with the direct EDFTs generated by one value of $\varphi = \varphi_1$ and the inverse EDFTs with angles $\varphi_2 \neq \varphi_1$.

Conclusions

In this paper, we describe the concept of the block-type elliptic discrete Fourier transforms, EDFT, in the real space R^{2N} . The proposed transform generalizes the traditional N -point DFT. The EDFT is based on the matrices that are roots of the identity matrix 2×2 which define rotations of the point around ellipses. The EDFT is parameterized and has a unique fast algorithm for any integer $N > 1$. The whole theory of the discrete Fourier transform and its application are based on the idea of rotating the data around circles. The EDFT is a general concept of rotating data around ellipses, and the DFT is a particular case of the EDFT. Our preliminary experimental results show that the EDFT together with the DFT can be used effectively in different areas of signal and image processing, including the filtration, enhancement of gray and color images, and encryption.